

# Simulation analysis of a high efficiency GaInP/Si multijunction solar cell

M. Benaicha<sup>1</sup>, L. Dehimi<sup>1,2</sup>, F. Pezzimenti<sup>3,†</sup>, and F. Bouzid<sup>4</sup>

<sup>1</sup>Laboratory of Metallic and Semiconductor Materials, University of Biskra, Biskra 07000, Algeria

<sup>2</sup>Faculty of Science, University of Batna, Batna 05000, Algeria

<sup>3</sup>DIIES - Mediterranean University of Reggio Calabria, Reggio Calabria 89122, Italy

<sup>4</sup>UDCMA - Research Center in Industrial Technologies, Algiers 16014, Algeria

**Abstract:** The solar power conversion efficiency of a gallium indium phosphide (GaInP)/silicon (Si) tandem solar cell has been investigated by means of a physical device simulator considering both mechanically stacked and monolithic structures. In particular, to interconnect the bottom and top sub-cells of the monolithic tandem, a gallium arsenide (GaAs)-based tunnel-junction, i.e. GaAs(n<sup>+</sup>)/GaAs(p<sup>+</sup>), which assures a low electrical resistance and an optically low-loss connection, has been considered. The  $J$ - $V$  characteristics of the single junction cells, monolithic tandem, and mechanically stacked structure have been calculated extracting the main photovoltaic parameters. An analysis of the tunnel-junction behaviour has been also developed. The mechanically stacked cell achieves an efficiency of 24.27% whereas the monolithic tandem reaches an efficiency of 31.11% under AM1.5 spectral conditions. External quantum efficiency simulations have evaluated the useful wavelength range. The results and discussion could be helpful in designing high efficiency monolithic multijunction GaInP/Si solar cells involving a thin GaAs(n<sup>+</sup>)/GaAs(p<sup>+</sup>) tunnel junction.

**Key words:** GaInP/Si; tandem solar cells; power efficiency; numerical simulations

**Citation:** M Benaicha, L Dehimi, F Pezzimenti, and F Bouzid, Simulation analysis of a high efficiency GaInP/Si multijunction solar cell[J]. *J. Semicond.*, 2020, 41(3), 032701. <http://doi.org/10.1088/1674-4926/41/3/032701>

## 1. Introduction

Solar photovoltaics (PV) is a continuously growing technology ascertained as one of the most promising candidates to reduce the fossil fuel energy demand for the next decades in a large number of space and terrestrial applications.

Nowadays the research on PV is focused on deploying new materials and/or complex device structures<sup>[1–9]</sup>. In this context, multijunction solar cells based on III–V semiconductors aid to compensate the spectral sensitivity by increasing the spectral absorption range<sup>[10, 11]</sup>. High efficiencies on the order of 43.5% have been already demonstrated for GaInP/GaAs/GaInNAs solar cells<sup>[12]</sup>. However, the optimizing solar cell performance with cost reduction remains a key issue for designers and the monolithic integration on silicon (Si) substrates is a practical way to reduce the manufacturing costs of tandem cells by reducing the cost of the starting material<sup>[13–17]</sup>.

In more detail, III–V/Si multijunction solar cells have achieved efficiencies around 30% for monolithic InGaN/Si two-junction structures<sup>[18]</sup>, and 35% for In<sub>0.46</sub>Ga<sub>0.54</sub>N/Si tandem solar cells<sup>[19]</sup>. In addition, simulation studies have showed that efficiencies in excess of 33% can be calculated for Al<sub>x</sub>Ga<sub>1–x</sub>As/epi-Si(Ge) solar cells<sup>[20]</sup>. At the same time, a mechanically stacked GaInP/Si tandem reaching an efficiency of 27% under 1 sun has been demonstrated in Ref. [21] by us-

ing an optimized structure that involves anti-reflection coating and passivation layers at the frontside of the top and bottom cell, respectively.

In this paper, both mechanically stacked and monolithic multijunction (MMJ) GaInP/Si solar cells are investigated. In particular, the sub-cells of the monolithic device are interconnected by considering a GaAs(n<sup>+</sup>)/GaAs(p<sup>+</sup>) tunnel-junction which allows, in principle, a current flow through the structure minimizing the voltage drops<sup>[22]</sup>. In fact, depending on the Ga composition, the In<sub>1–x</sub>Ga<sub>x</sub>P alloy can be grown on a GaAs substrate with an appropriate lattice match as investigated experimentally in Ref. [23]. The choice of a GaAs(n<sup>+</sup>)/GaAs(p<sup>+</sup>) tunnel-junction in designing a III–V/Si multijunction solar cell is also supported by our previous study presented in Ref. [19].

The fundamental PV parameters, such as the open circuit voltage ( $V_{oc}$ ), short circuit current density ( $J_{sc}$ ), fill factor (FF), and conversion efficiency ( $\eta$ ) have been calculated under AM1.5 spectral conditions. In particular, the mechanically stacked tandem and the monolithic tandem achieve an efficiency of 24.27% and 31.11%, respectively.

## 2. Device structure and modelling

The schematic cross-section of the proposed MMJ GaInP/Si solar cell is shown in Fig. 1. The drawing is not to scale.

We consider a GaInP top-cell, with a material bandgap energy of 1.8 eV, and a conventional Si bottom-cell connected in series by means of a GaAs(n<sup>+</sup>)/GaAs(p<sup>+</sup>) tunnel-junction. Detailed information for the different layers is given in Table 1.

Correspondence to: F Pezzimenti, [fortunato.pezzimenti@unirc.it](mailto:fortunato.pezzimenti@unirc.it)

Received 27 MAY 2019; Revised 24 OCTOBER 2019.

©2020 Chinese Institute of Electronics

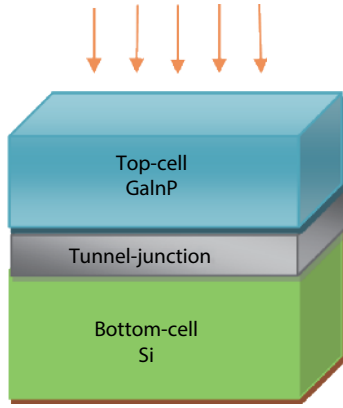


Fig. 1. (Color online) Schematic cross-section of the MMJ GaInP/Si solar cell.

Table 1. Structure of the simulated GaInP/Si MMJ tandem cell.

Parameter	Material	Role	Thickness ( $\mu\text{m}$ )	Net doping ( $\text{cm}^{-3}$ )
Top-cell	AlInP (n)	Window	0.02	$2 \times 10^{18}$
	GaInP (p)	Emitter	1.00	$5 \times 10^{17}$
	GaInP (n)	Base	0.03	$1 \times 10^{16}$
	$\text{Al}_{0.25}\text{Ga}_{0.25}\text{P}$	BSF	0.02	$2 \times 10^{18}$
Tunnel-junction	$\text{In}_{0.5}\text{P}$ (p)	$n^{++}$ layer	0.025	$5 \times 10^{19}$
	GaAs ( $n^{+}$ )	$p^{++}$ layer	0.025	$5 \times 10^{19}$
Bottom-cell	Si (n)	Emitter	3	$5 \times 10^{17}$
	Si (p)	Base	180	$5 \times 10^{17}$

In the top-cell, the back-surface field (BSF) layer and the window layer are assumed to reduce the surface recombination velocity and the scattering of carriers towards the tunnel-junction (TJ), respectively. These two layers have the same thickness (20 nm) and net doping ( $2 \times 10^{18} \text{ cm}^{-3}$ ). The TJ is a highly doped ( $5 \times 10^{19} \text{ cm}^{-3}$ ) ultra-thin layer with a thickness of 50 nm. This TJ structure has been already investigated in Ref. [19] appearing, with an overall thickness in the limit of 60 nm, well suited for the design of high efficiency III-V/Si multijunction solar cells.

The modelling activity has been performed by using the Silvaco-TCAD numerical simulation software to solve Poisson's equation and continuity equations for carriers under steady state conditions. The solar cell has been investigated under AM1.5 radiation ( $100 \text{ mW/cm}^2$ ) and photons are assumed to be incident from the p-GaInP side of the GaInP top-cell. Recent papers addressing the modelling of different devices support the considered simulation setup as briefly recalled in the following [24–27]. In particular, it involves the effective density of states, and the doping-dependent recombination processes and carrier mobilities. Also, specific expressions depending on In composition in the GaInP regions, such as the bandgap energy, electron affinity, and relative permittivity, are taken into account.

The fundamental  $\text{In}_x\text{Ga}_{1-x}\text{P}$  material parameters are calculated using the physical models summarized in Table 2.

Two of the most critical parameters for advanced solar cell modelling are the material refractive index,  $n$ , and the extinction coefficient,  $K$ . Because of the difficulty in collecting optical parameters for many ternary and quaternary materials, a good approximation of  $n$  and  $K$  may be obtained by interpolating simpler compounds data. In particular, the interpolation between the GaP and InP data allows to estimate the op-

Table 2. Physical models.

Parameter	Expression
Bandgap energy <sup>[28, 29]</sup>	$E_g(x) = -0.272x^2 + 1.19x - 1.34$
Electron affinity <sup>[30]</sup>	$\chi(x) = 4.38 - 0.58x$
Relative permittivity <sup>[31]</sup>	$\epsilon_s(x) = 12.5 - 1.4x$
Effective density of states <sup>[31, 32]</sup>	$N_{c,v} = 2 \left( \frac{\pi q K T m_{e,h}^*}{h^2} \right)^{3/2}$
Carrier mobility <sup>[10, 31]</sup>	$\mu_n = \frac{4000}{1 + \left( \frac{N}{1 \times 10^{15}} \right)^{0.27}}, \mu_p = 40 \text{ cm}^2/(\text{V} \cdot \text{s})$

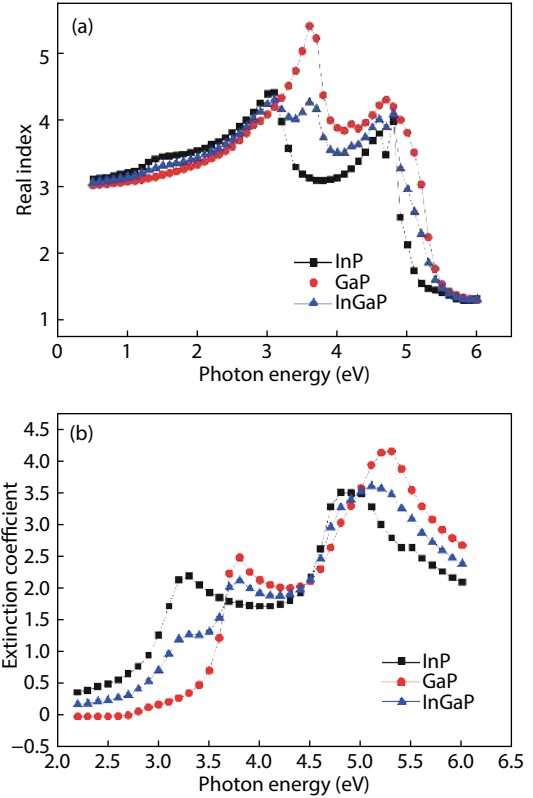


Fig. 2. (Color online) Interpolation of (a)  $n$  and (b)  $K$  for  $\text{Ga}_{0.5}\text{In}_{0.5}\text{P}$ .

tical parameters for the  $\text{Ga}_{0.5}\text{In}_{0.5}\text{P}$  compound as shown in Fig. 2<sup>[33]</sup>.

Finally, the absorption coefficient for the Si substrate is calculated by the following expressions<sup>[34]</sup>:

$$\alpha_{\text{Si}} = -0.425(E - E_g)^3 + 0.757(E - E_g)^2 - 0.0224(E - E_g), \quad (1)$$

$$\alpha_{\text{Si}} = 0.0287 \exp[2.72(E - E_g)], \quad (2)$$

for  $1.12 \leq E < 1.5 \text{ eV}$  and  $E \geq 1.5 \text{ eV}$ , respectively.

### 3. Tunnel-junction behaviour

In multijunction solar cells, the TJ shorts the n/p regions of the adjacent sub-cells and the tandem structure can be de facto treated as a single junction cell<sup>[35]</sup>. Nowadays, the TJ plays a key role once the photocurrent losses from light absorption in this region are minimized. In other words, the TJ design should be transparent to the wavelengths absorbed by the series-connected sub-cells and also forming a low-resistive interface which assures minimal voltage drops.

Basically, the TJ is a degenerately doped p/n junction

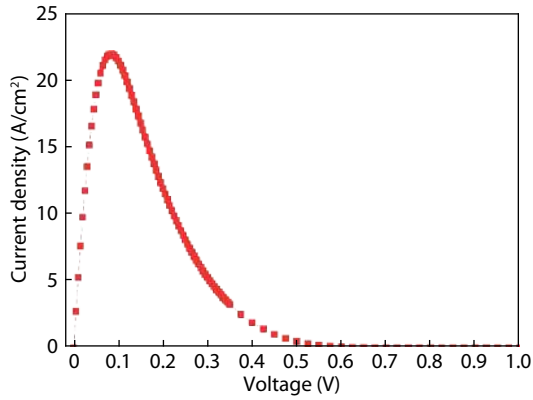


Fig. 3. (Color online)  $J$ - $V$  curve of the GaAs(n+)/GaAs(p<sup>+</sup>) TJ in dark.

which leads to quantum tunneling phenomena for electrons in forward-bias. The relative expression of the current density is the form of Ref. [22],

$$J(E) = \frac{qkTm^*}{2\pi^2\hbar^3} T(E) \ln \left( \frac{1 + \exp(E_{FL} - E)/kT}{1 + \exp(E_{FR} - E)/kT} \right) \Delta E, \quad (3)$$

where  $E_{FR}$  and  $E_{FL}$  are the Fermi levels in the valence and conduction band, respectively, and  $T(E)$  is the tunneling probability expressed by the Wentzel–Kramers–Brillouin theory assuming the electron wave function  $k(x)$  as an exponential term integrated over the depletion region as follows:

$$T(E) \approx \exp \left[ -2 \int_{-x_1}^{x_2} |k(x)| dx \right]. \quad (4)$$

Here,  $x_1$  and  $x_2$  are the edges of the depletion region.

As introduced in the previous section, in this study we have considered a highly doped GaAs(n<sup>+</sup>)/GaAs(p<sup>+</sup>) TJ between the GaInP and Si regions of the GaInP/Si MMJ solar cell. This improves the cell efficiency as discussed in Refs. [29, 35]. The simulated  $J$ - $V$  curve of the TJ in dark is shown in Fig. 3.

The design structure has a peak of the tunneling current density close to 22 A/cm<sup>2</sup>. This value has to be higher than the  $J_{sc}$  value of the relative solar cell to satisfy the so called “first criteria” for the MMJ design<sup>[36]</sup>. Moreover, a resistance as low as 4 mΩ·cm<sup>2</sup> can be calculated from Fig. 3 at the aforementioned current density.

## 4. Results and discussion

### 4.1. GaInP and Si single cells

The proposed multijunction cell is structured with two stacked GaInP and Si cells. These two cells are firstly investigated individually. This way, their electrical characteristics have been properly adjusted and the resulting  $J$ - $V$  curves are shown in Fig. 4.

The PV parameters extracted for each cell, namely the open circuit voltage,  $V_{oc}$ , the short circuit current density,  $J_{sc}$ , the fill factor, FF, and the conversion efficiency,  $\eta$ , are listed in Table 3. As we can see, due to the material wide bandgap, the GaInP single cell generates a large  $V_{oc}$  of 1.45 V and a  $J_{sc}$  of 16.75 mA/cm<sup>2</sup>. These values are in good agreement with those measured in Ref. [37] where a comparable GaInP single junction solar cell with  $\eta = 20.8\%$  has been characterized.

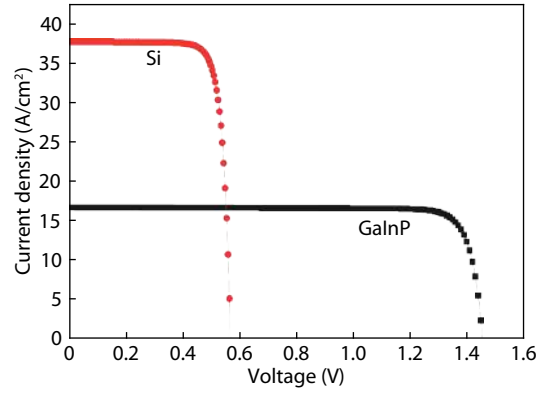


Fig. 4. (Color online)  $J$ - $V$  characteristics of the Si and GaInP single cells.

Table 3. PV parameters extracted from Fig. 4.

Parameter	$J_{sc}$ (mA/cm <sup>2</sup> )	$V_{oc}$ (V)	FF (%)	$\eta$ (%)
GaInP single-cell	16.75	1.45	86.11	20.99
Si single-cell	37.7	0.56	81.27	17.45

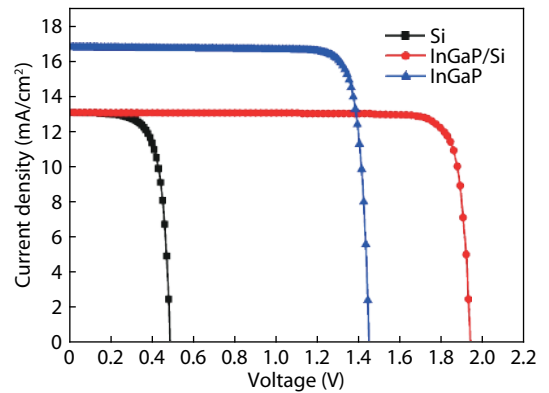


Fig. 5. (Color online)  $J$ - $V$  curve for both the single junction cells and the InGaP tandem structure.

Also, they validate the adopted simulation setup in providing reliable results with an error in the conversion efficiency calculation associated to the uncertainty of some simulation parameters which is in the limit of 0.5%. This range of variability is consistent with the results reported in Ref. [21].

### 4.2. Mechanically stacked structure

In this section, we present the simulation results obtained when the GaInP and Si solar cells are next placed in a mechanically stacked configuration by means of a transparent adhesive layer. The  $J$ - $V$  behaviour for both the single junction cells and the tandem structure are shown in Fig. 5.

As expected, the  $J$ - $V$  curve of the top-cell is unaffected and it appears as in Fig. 4. Contrariwise, the bottom-cell produces less current due to fact that higher energy photons are absorbed by the top-cell. From Fig. 5, the extracted PV parameters are listed in Table 4.

To obtain detailed information about the useful wavelength range in the tandem structure, external quantum efficiency (EQE) simulations have been performed. The EQE of the GaInP top-cell and Si bottom-cell under 1-sun AM1.5 illumination is shown in Fig. 6.

As we can see, the top-cell has a greater collection efficiency for carriers generated by shorter wavelengths while the bottom-cell has a greater collection efficiency for carriers

Table 4. PV parameters extracted from Fig. 5.

Parameter	$J_{sc}$ (mA/cm <sup>2</sup> )	$V_{oc}$ (V)	FF (%)	$\eta$ (%)
GaInP top-cell	16.75	1.45	86.11	20.99
Si bottom-cell	13.06	0.48	71.24	3.28
GaInP/Si tandem cell	13.06	1.93	96.9	24.27

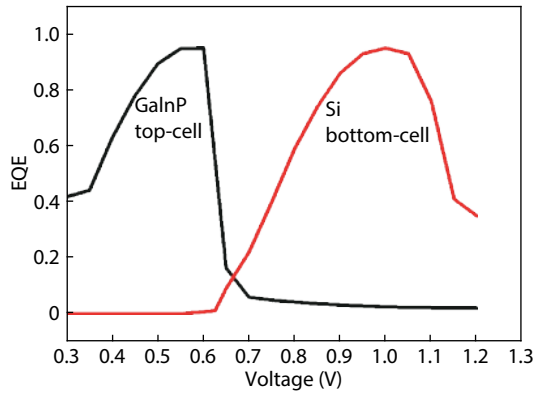


Fig. 6. (Color online) EQE of the GaInP top-cell and Si bottom-cell in the stacked structure.

generated by longer wavelengths. Therefore, these two cells can be considered complementary in a tandem structure although an optimized design in terms of geometrical and physical parameters should be also addressed to the shrinkage of the EQE transition region as much as possible. For example, in Fig. 6, the EQE is limited to about 0.2 in the wavelength range from 0.65 to 0.7  $\mu\text{m}$ .

### 4.3. Multi-junction solar cell

By placing the GaAs(n<sup>+</sup>)/GaAs(p<sup>+</sup>) TJ in the vertical stacking of the GaInP and Si single cells, we can investigate the MMJ structure. The corresponding band diagram of the GaInP/Si tandem cell at thermodynamic equilibrium is shown in Fig. 7(a). In this bias condition, the electron quasi Fermi level (QFL) is a constant across the structure.

We can note that the TJ is located around 1.15  $\mu\text{m}$  from the top surface and in fact, at this depth, the electric field profile along the cell exhibits a peak value as high as 3.5 MV/cm as shown in Fig. 7(b).

Here, the energy levels behaviours originate a tunnel region that leads to carrier recombination phenomena. In other words, the band energy levels bend sufficiently to allow carriers to tunnel by internal field emission.

Finally, the simulated  $J$ - $V$  curve of the MMJ solar cell is shown in Fig. 8. Here, the current behaviour of the mechanical stacked structure in Fig. 5 is also reported for comparison. The extracted PV parameters are summarized in Table 5.

We obtain a conversion efficiency of 31.11% for the MMJ structure involving an optimized tunnel junction, which is higher than 24.27% calculated for the mechanically stacked cell.

It is worthwhile noting that, by comparing the simulation results of the mechanically stacked cell with respect to the measurements reported in Ref. [21] for a mechanically stacked 4-terminal GaInP/Si tandem cell performing a conversion efficiency close to 27%, the resulting efficiency difference (about 2 percentage-points) is mainly due to the performance of the conventional Si-based bottom cell. In fact, since the optimized design of the Si single cell was not investigated in this work, before stacking it achieves 17.45% as reported

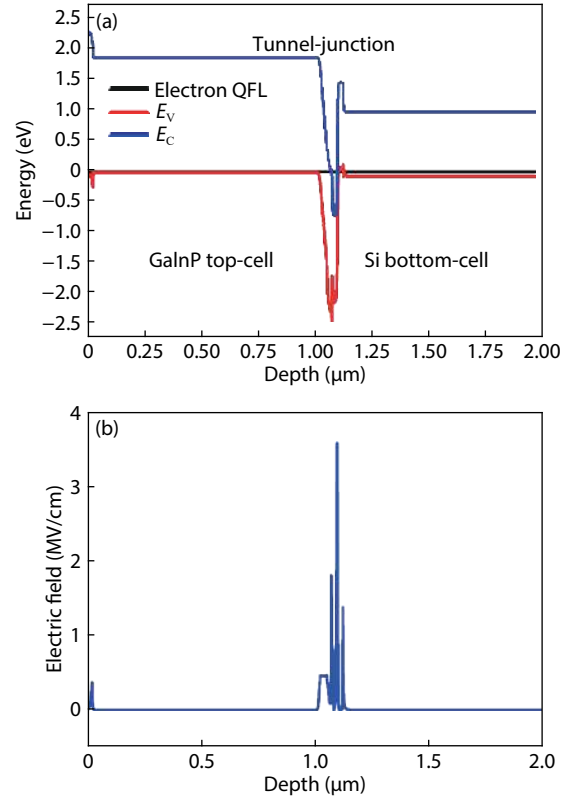
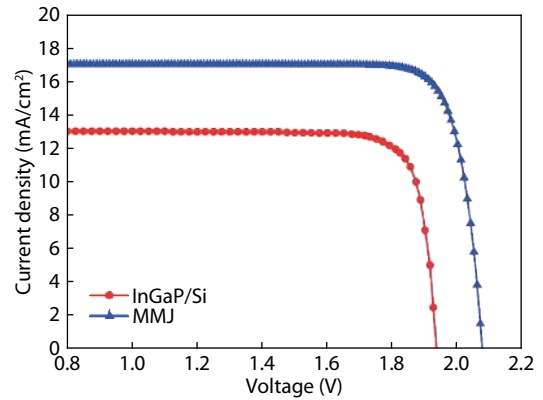
Fig. 7. (Color online) (a) Energy band diagram of the GaInP/Si tandem cell at thermodynamic equilibrium;  $E_v$  and  $E_c$  are the energy levels of the valence and conduction band, respectively. (b) Electric field profile.Fig. 8. (Color online) Comparison between the  $J$ - $V$  curves of the MMJ tandem cell and the GaInP/Si mechanical stacked structure.

Table 5. PV parameters of the proposed GaInP/Si tandem solar cells.

Parameter	$J_{sc}$ (mA/cm <sup>2</sup> )	$V_{oc}$ (V)	FF (%)	$\eta$ (%)
MMJ cell	17.04	2.07	87.99	31.11
Mechanical stacked cell	13.06	1.93	96.9	24.27

in Table 3 against 19.7% in Ref. [21] where anti-reflection coating and passivation layers are added at the frontside for optimization.

## 5. Conclusion

In this paper GaInP/Si tandem solar cells have been analysed by using a physical device simulator. During the simulations, we considered both mechanically stacked and monolithic multi-junction structures that involve a relative thin GaAs(n<sup>+</sup>)/GaAs(p<sup>+</sup>) tunnel junction. By extracting the main

photovoltaic parameters from the  $J$ - $V$  curves, the first design shows an efficiency of 24.27% whereas the latter achieves an efficiency of 31.11% under AM1.5 spectral conditions. The obtained results have been compared with literature data to validate the adopted simulation setup in providing reliable results that avoid an overestimation of the model in the calculation of the PV parameters. The developed analysis could be the theoretical basis for the design of high efficiency MMJ GaInP/Si solar cells with an optimized GaAs(n<sup>+</sup>)/GaAs(p<sup>+</sup>) tunnel junction.

## References

- [1] Asadpour R, Chavali R V K, Khan M R, et al. Bifacial Si heterojunction-perovskite organic-inorganic tandem to produce highly efficient ( $\eta_T^* \sim 33\%$ ) solar cell. *Appl Phys Lett*, 2015, 106, 243902
- [2] Bencherif H, Dehimi L, Pezzimenti F, et al. Multiobjective optimization of design of 4H-SiC power MOSFETs for specific applications. *J Electron Mater*, 2019, 48, 3871
- [3] De Martino G, Pezzimenti F, Della Corte F G. Interface trap effects in the design of a 4H-SiC MOSFET for low voltage applications. Proc International Semiconductor Conference – CAS, 2018: 147
- [4] Bouzid F, Dehimi L, Pezzimenti F, et al. Numerical simulation study of a high efficient AlGaIn-based ultraviolet photodetector. *Superlattice Microstruct*, 2018, 122, 57
- [5] Bouzid F, Dehimi L, Pezzimenti F. Performance analysis of a Pt/n-GaN Schottky barrier UV detector. *J Electron Mater*, 2017, 46, 6563
- [6] Megherbi M L, Pezzimenti F, Dehimi L, et al. Analysis of the forward  $I$ - $V$  characteristics of Al-implanted 4H-SiC p-i-n diodes with modeling of recombination and trapping effects due to intrinsic and doping-induced defect states. *J Electron Mater*, 2018, 47, 1414
- [7] Fritah A, Dehimi L, Pezzimenti F, et al. Analysis of  $I$ - $V$ - $T$  characteristics of Au/n-InP Schottky barrier diodes with modeling of nanometer-sized patches at low temperature. *J Electron Mater*, 2019, 48, 3692
- [8] Megherbi M L, Pezzimenti F, Dehimi L, et al. Analysis of trapping effects on the forward current-voltage characteristics of Al-implanted 4H-SiC p-i-n diodes. *IEEE Trans Electron Devices*, 2018, 65, 3371
- [9] Bencherif H, Dehimi L, Pezzimenti F, et al. Temperature and SiO<sub>2</sub>/4H-SiC interface trap effects on the electrical characteristics of low breakdown voltage MOSFETs. *Appl Phys A*, 2019, 125, 294
- [10] Olson J M, Friedman D J, Kurtz S. High efficiency III-V multi-junction solar cells. In: Handbook of Photovoltaic Science and Engineering. New York: John Wiley & Sons, 2003
- [11] Zheng Y, Mihara A, Yamamoto A. Analysis of In<sub>x</sub>Ga<sub>1-x</sub>N/Si p-n heterojunction solar cells and the effects of spontaneous and piezoelectric polarization charges. *Appl Phys Lett*, 2013, 103, 153509
- [12] Green M A, Emery K, Hishikawa Y, et al. Solar cell efficiency tables (ver. 39). *Prog Photovolt: Res Appl*, 2012, 20, 12
- [13] Connolly J P, Mencaraglia D, Renard C, et al. Designing III-V multijunction solar cells on silicon. *Prog Photovolt: Res Appl*, 2014, 22, 810
- [14] Bencherif H, Dehimi L, Pezzimenti F, et al. Improving the efficiency of a-Si: H/c-Si thin heterojunction solar cells by using both antireflection coating engineering and diffraction grating. *Optik*, 2019, 182, 682
- [15] Green M A. Silicon wafer-based tandem cells: The ultimate photovoltaic solution. Proc SPIE Physics, Simulation, and Photonic Engineering of Photovoltaic Devices III, 2014: 89810
- [16] Bencherif H, Dehimi L, Pezzimenti F, et al. Analytical model for the light trapping effect on ZnO: Al/c-Si/SiGe/c-Si solar cells with an optimized design. Proc 2018 International Conference on Applied Smart Systems, ICASS, 2019, 8651990
- [17] Liu H, Ren Z, Liu Z, et al. The realistic energy yield potential of GaAs on Si tandem solar cells: a theoretical case study. *Opt Express*, 2015, 23, 382
- [18] Hsu L, Walukiewicz W. Modeling of InGaN/Si tandem solar cells. *J Appl Phys*, 2008, 104, 024507
- [19] Benaicha M, Dehimi L, Sengouga N. Simulation of double junction InGaIn/Si tandem solar cell. *J Semicond*, 2017, 38, 044002
- [20] Lachaume R, Carioub R, Decobertb J, et al. Performance analysis of Al<sub>x</sub>GaAs/epi-Si(Ge) tandem solar cells: a simulation study. *Energy Procedia*, 2015, 84, 41
- [21] Essig S, Ward S, Steiner M A. Progress towards a 30% efficient GaInP/Si tandem solar cell. *Energy Procedia*, 2015, 77, 464
- [22] Baudrit M, Algora C. Theoretical optimization of GaInP/GaAs dual-junction solar cell: Toward a 36% efficiency at 1000 suns. *Phys Status Solidi A*, 2010, 207, 474
- [23] Kinacı B, Özen Y, Asar T, et al. Effect of alloy composition on structural, optical and morphological properties and electrical characteristics of Ga<sub>x</sub>In<sub>1-x</sub>P/GaAs structure. *J Mater Sci Mater Electron*, 2013, 24, 3269
- [24] Marouf Y, Dehimi L, Bouzid F, et al. Theoretical design and performance of In<sub>x</sub>Ga<sub>1-x</sub>N single junction solar cell. *Optik*, 2018, 163, 22
- [25] Bouzid F, Pezzimenti F, Dehimi L, et al. Numerical simulations of the electrical transport characteristics of a Pt/n-GaN Schottky diode. *Jpn J Appl Phys*, 2017, 56, 094301
- [26] Zeghdar K, L Dehimi L, Pezzimenti F, et al. Simulation and analysis of the current-voltage-temperature characteristics of Al/Ti/4H-SiC Schottky barrier diodes. *Jpn J Appl Phys*, 2019, 58, 014002
- [27] Marouf Y, Dehimi L, Pezzimenti F. Simulation study for the current matching optimization in In<sub>0.48</sub>Ga<sub>0.52</sub>N/In<sub>0.74</sub>Ga<sub>0.26</sub>N dual junction solar cells. *Superlattice Microstruct*, 2019, 130, 377
- [28] Walker A W, Wheeldon J F, Valdivia C E, et al. Simulation, modeling and comparison of III-V tunnel junction designs for high efficiency metamorphic multi-junction solar cells. Proc of SPIE, Photonics North, 2010: 7750
- [29] Bouzid F, Pezzimenti F, Dehimi L, et al. Analytical modeling of dual-junction tandem solar cells based on an InGaP/GaAs heterojunction stacked on a Ge substrate. *J Electron Materials*, 2019, 48, 4107
- [30] Haas A, Wilcox J, Gray J, et al. Design of A GaInP/GaAs tandem solar cell for maximum daily, monthly, and yearly energy output. *J Photon Energy*, 2011, 1, 180011
- [31] Goldberg Y A. Handbook series on semiconductor parameters. Vol. 2. London: World Scientific, 1999
- [32] Brozel M R, Stillman G E. Properties of gallium arsenide. 3rd ed. London: Institution of Electrical Engineers, 1996
- [33] Adachi S. Optical constants of semiconductors in tables and figures: Handbook. London: World Scientific, 2012
- [34] Sze S M. Physics of semiconductor devices. 2nd ed. New York: John Wiley & Sons, 2001
- [35] Michael S, Lavery J. Multi-junction photovoltaic model optimization for space and solar concentrator applications. Proc 23rd European Photovoltaic Solar Energy Conference, 2008, 790
- [36] Hegedus S. Handbook of photovoltaic science and engineering. New York: John Wiley & Sons, 2003
- [37] Geisz J F, Steiner M A, I Garcia I, et al. Enhanced external radiative efficiency for 20.8% efficient single-junction GaInP solar cells. *Appl Phys Lett*, 2013, 103, 0411181